# Characterizations of nonlinear optical properties on GaN crystals in polar, nonpolar, and semipolar orientations

Hong Chen, , Xuanqi Huang, , Houqiang Fu, , Zhijian Lu, , Xiaodong Zhang, , Jossue A. Montes, and , and Yuji Zhao

Citation: Appl. Phys. Lett. **110**, 181110 (2017); doi: 10.1063/1.4983026
View online: http://dx.doi.org/10.1063/1.4983026
View Table of Contents: http://aip.scitation.org/toc/apl/110/18
Published by the American Institute of Physics

**Articles you may be interested in**

Demonstration of a mid-wavelength infrared narrowband thermal emitter based on GaN/AlGaN quantum wells and a photonic crystal
Applied Physics Letters **110**, 181109 (2017); 10.1063/1.4983020

Nonpolar and semipolar InGaN/GaN multiple-quantum-well solar cells with improved carrier collection efficiency
Applied Physics Letters **110**, 161105 (2017); 10.1063/1.4980139

Ultraviolet light-absorbing and emitting diodes consisting of a p-type transparent-semiconducting NiO film deposited on an n-type GaN homoepitaxial layer
Applied Physics Letters **110**, 181102 (2017); 10.1063/1.4982653

Electron mobility in polarization-doped $Al_{0-0.2}GaN$ with a low concentration near $10^{17}$ $cm^{-3}$
Applied Physics Letters **110**, 182102 (2017); 10.1063/1.4982920

Thin-film GaN Schottky diodes formed by epitaxial lift-off
Applied Physics Letters **110**, 173503 (2017); 10.1063/1.4982250

150 mW deep-ultraviolet light-emitting diodes with large-area AlN nanophotonic light-extraction structure emitting at 265 nm
Applied Physics Letters **110**, 141106 (2017); 10.1063/1.4978855

# Characterizations of nonlinear optical properties on GaN crystals in polar, nonpolar, and semipolar orientations

Hong Chen, Xuanqi Huang, Houqiang Fu, Zhijian Lu, Xiaodong Zhang, Jossue A. Montes, and Yuji Zhao[a)]

*School of Electrical, Computer and Energy Engineering, Arizona State University, Tempe, Arizona 85287, USA*

(Received 21 February 2017; accepted 22 April 2017; published online 3 May 2017)

We report the basic nonlinear optical properties, namely, two-photon absorption coefficient (β), three-photon absorption coefficient (γ), and Kerr nonlinear refractive index ($n_{kerr}$), of GaN crystals in polar *c*-plane, nonpolar *m*-plane, and semipolar ($20\bar{2}1$) plane orientations. A typical Z-scan technique was used for the measurement with a femtosecond Ti:S laser from wavelengths of 724 nm to 840 nm. For the two-photon absorption coefficient (β), similar values were obtained for polar, nonpolar, and semipolar samples, which are characterized to be ~0.90 cm/GW at 724 nm and ~0.65 cm/GW at 730 nm for all the three samples. For the Kerr nonlinear refractive index ($n_{kerr}$), self-focusing features were observed in this work, which is different from previous reports where self-defocusing features were observed on GaN in the visible and near-UV spectral regions. At 724 nm, $n_{kerr}$ was measured to be $\sim 2.5\,0 \times 10^{-14}\,cm^2/W$ for all three samples. Three-photon absorption coefficients (γ) were also determined, which were found to be consistent with previous reports. This study provides valuable information on the basic nonlinear optical properties of III-nitride semiconductors, which are vital for a wide range of applications such as integrated photonics and quantum photonics. *Published by AIP Publishing.* [http://dx.doi.org/10.1063/1.4983026]

III-nitride semiconductors have drawn considerable attention for their wide range of applications in solid-state lighting,[1–3] solar cells,[4] high-speed visible light communication,[5] and intersubband transition optoelectronic devices.[6,7] In addition to these applications, recent studies on III-nitride based waveguides have opened new opportunities due to their wide bandgap, low material dispersion, and active integration capability,[8] which are particularly attractive for applications in nonlinear optics,[9–13] including second harmonic generation,[9,13] comb generation,[10,11] and parametric down conversion.[12] For example, in nonlinear processes where high pumping power density is required (second harmonic generation[9,13] and parametric down conversion[12]) or in resonators which require high quality factors (ring resonators[9–12] and microdisk resonators[13,14]), the nonlinear absorption contributed by multi-photon absorption plays a significant role in the processes and must be considered. Despite their importance, there have been only very few reports on the basic nonlinear properties of III-nitride materials, e.g., the two photon absorption (TPA) coefficient (β), Kerr refractive index ($n_{kerr}$), and three photon absorption (3PA) coefficient (γ).[15–18] Sun *et al.* studied TPA coefficients above half-bandgap photon energy for polar *c*-plane GaN, where the TPA coefficients β were reported to be 17±7 and 14±6 cm/GW at 387 and 391 nm, respectively, and 3±1.5 and 7±3 cm/GW at 720 and 690 nm, respectively.[15] Furthermore, Fang *et al.* showed $n_{kerr} = 1.15 \times 10^{-14}\,cm^2/W$ (E⊥c) and $1.4 \times 10^{-14}\,cm^2/W$ (E ∥ c) at 800 nm for *c*-plane bulk GaN.[18] These results, however, have been almost exclusively focused on conventional polar *c*-plane III-nitrides. Recently, a new class of III-nitride materials, namely, nonpolar and semipolar III-nitrides, have emerged with very different material and optical properties, leading to distinct device performance for light-emitting devices and solar cells.[1–7] In this work, we perform a comprehensive characterization on the TPA coefficient β, $n_{kerr}$, and 3PA coefficient γ, for bulk GaN in polar, nonpolar, and semipolar orientations, which have never been fully studied.

Commercial double polished bulk GaN substrates on the polar *c*-plane, nonpolar *m*-plane, and semipolar ($20\bar{2}1$) plane were used for the study. The substrates were grown using the hydride vapor phase epitaxy (HVPE) method with a dislocation density of $2 \times 10^5 - 2 \times 10^6\,cm^{-3}$. A typical Z-scan method[19,20] was used for the optical characterization, and the schematic of the setup is shown in Fig. 1(a). A femtosecond Ti:S laser was tuned from 724 nm to 840 nm in the femtosecond pulsed mode, and the typical spectrum of the laser used in this research is shown in Fig. 1(b). A light beam was focused using a ×20 microscope objective, and the Rayleigh range and beam size were extracted from the fitting of experimental data (shown in Fig. 1(c)) using following equations:[20]

$$T \approx 1 - \frac{\beta I_0 L_{eff}}{2\sqrt{2}} \times \frac{1}{1 + Z^2/Z_0^2}, \tag{1}$$

$$Z_0 = \frac{n\pi\omega_0^2}{\lambda}, \tag{2}$$

where $T$ is the normalized transmission, $I_0$ is the peak beam power density, $L_{eff}$ is the effective sample length, $Z_0$ is the Rayleigh range of the beam, $n$ is the refractive index, $\omega_0$ is the beam size at the focal plane, and $\lambda$ is the wavelength. $L$ is the sample thickness, and in this work, $L_{eff} \approx L \approx 500\,\mu m$. The samples are sufficiently thick such that the Fabry–Pérot

a)Email: yuji.zhao@asu.edu

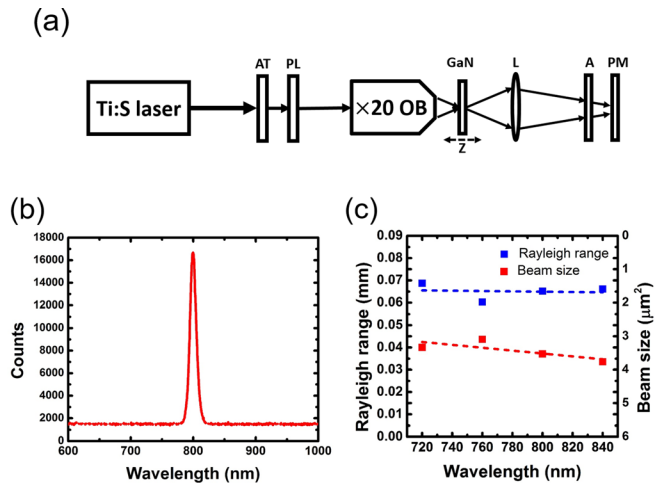


FIG. 1. (a) Schematic figure of the experimental setup: "AT" is the beam attenuator, "PL" is the polarizer, "OB" is the microscope objective, "L" is the lens, "A" is the aperture, **and** "PM" is the power meter. (b) A typical spectrum for the laser used in this study. (c) Rayleigh range and the beam size estimated from the open aperture fitting.

(FP) resonance does not influence the results. Figure 1(c) shows the Rayleigh range and the beam size vs. wavelength for the measurement where the Rayleigh range remains constant within the spectrum, which indicates the invariant beam size during the measurement. For the open aperture measurement, all of the light was collected by using a power meter. For the closed aperture measurement, the aperture was tuned to allow 36% of the total power to pass through. The output power of the laser was kept stable in the pulsed mode, and therefore, a feedback loop was not required in this experiment to stabilize the incident power. We also need to note that, since unintentionally doped GaN possess a n-type conductivity[21] with a free carrier concentration of around $10^{17}\,\mathrm{cm}^{-3}$, using an analytical Drude model,[22] the free carrier absorption induced at this carrier density is estimated to be ~0.09 dB/cm at 800 nm, indicating >0.25% total optical power loss when propagating through the GaN slab. This loss is relatively small compared with multi-photon absorption induced optical loss shown in this work.

Figures 2(a)–2(c) show the open aperture and closed aperture plots for samples on the polar *c*-plane, nonpolar *m*-plane, and semipolar $(20\bar{2}1)$ plane, respectively. The peak beam power density was kept around $9\,\mathrm{GW/cm}^2$. For the characterization on the *m*- and $(20\bar{2}1)$-plane GaN, light is polarized along the *c* ($\mathrm{E} \| c$) and $[1\bar{2}1\bar{4}]$ (*c* projection, $\mathrm{E} \| c'$) direction, respectively, while for the *c*-plane, light is polarized on the *m* axis ($\mathrm{E} \| m$). For photons with energy larger than half bandgap (corresponding to $\lambda < 30$ nm), the TPA process was considered when fitting the open aperture curve. For photons with energy lower than half bandgap, the 3PA process was considered. The fitting results agree sufficiently well with the experimental data.

Figure 3(a) shows the transmission difference $\Delta T$ obtained from open aperture measurement for three samples. For simplicity, we fitted the points in "region I" only considering the TPA mechanism from the valence band (VB) to the conduction band (CB). We note that other mechanisms might also be responsible for the transmission change at the focal plane, e.g., 3PA, the Raman effect, and the Stark effect.[23] In "region II," we considered 3PA as the major mechanism responsible for the transmission change. The schematic for the dominant transitions in "region I" and "region II" is shown in Fig. 3(b). Strong yellow luminescence was observed throughout the experiment, which is possibly due to the deep level defect states in GaN.[24]

Figure 3(c) shows the TPA coefficient β vs. wavelength for the measurement, where the experimental results from previous studies were also plotted for comparison. A theoretical model developed by Sheik-Bahae was used to fit the data.[23] The TPA coefficient β is given by the following equation:

$$\beta(\omega) = K\frac{\sqrt{E_p}}{n_0^2 E_g^3} F_2\left(\mathrm{hbar}\cdot\omega/E_g\right), \tag{3}$$

where $E_g$ is the bandgap energy and $E_p = 2|P_{vc}|^2/m_0$, obtained by the $k\cdot p$ model, which is a material-independent parameter for direct bandgap semiconductors. $n_0$ is the refractive index, $\omega$ is the frequency, and $K$ is a material-independent constant. $F_2$ is a function with the form $F_2(x) = (2x-1)^{1.5}/(2x)^5$. The details of the approach can be found in Ref. 23. The β obtained from this study agrees well with the theoretical fitting and shows a consistent trend with the previous experimental results. The 3PA coefficient γ was obtained using the equation $\Delta\alpha = \gamma I_0^2$, and the results are summarized in Table I.

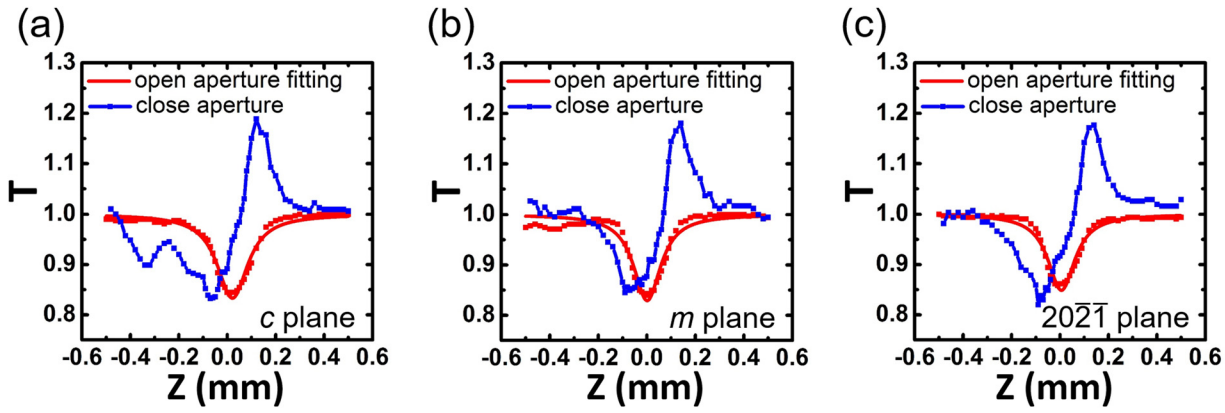


FIG. 2. The open aperture and closed aperture plots for samples on (a) the polar *c*-plane, (b) the nonpolar *m*-plane, and (c) the semipolar $(20\bar{2}1)$ plane. The results are measured at 724 nm incident light.

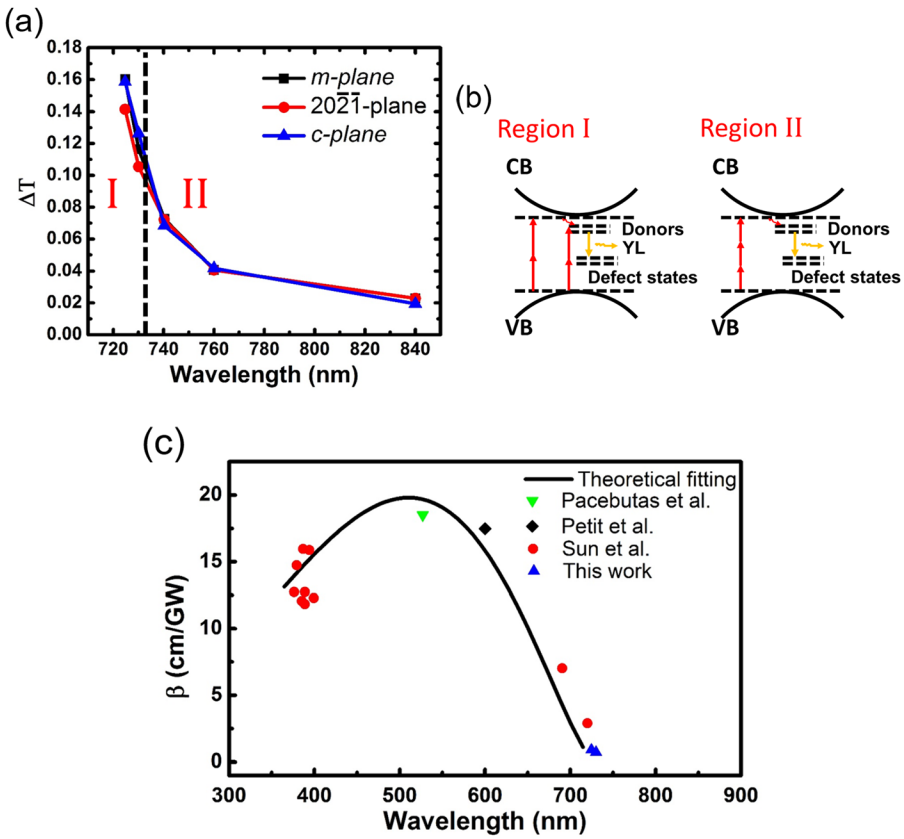


FIG. 3. (a) The transmission difference $\Delta T$ obtained from open aperture measurement for the three samples. (b) The schematic for the dominant transitions in "region I" and "region II." (c) The TPA coefficient $\beta$ vs. wavelength for the measurement is shown, and the experimental results from previous studies were also plotted for comparison. A theoretical model developed by Sheik-Bahae was used to fit the data.[22] Reproduced with permission from Appl. Phys. Lett. **76**, 439 (2000). Copyright 2000 AIP Publishing LLC.

In comparison with another wide-bandgap material SiN, the TPA coefficient $\beta$ is given as[25] $\sim 1.6 \times 10^4$ cm/GW at 800 nm. The value of β for GaN we obtained in this work is found to be four magnitudes lower, and we expect an even lower value for β on AlN. The low TPA coefficients make the III-nitride a very attractive material system for the fabrication of high quality second harmonic generators or entangled photon pair generators in the visible or even UV regions. Using the β and γ coefficients obtained above, we can briefly evaluate the performance of the GaN waveguide for nonlinear optics applications. For example, for a GaN waveguide with a mode area of 1 $\mu$m$^2$, if the optical power inside the waveguide is 1 mW, considering the CW operation condition, the nonlinear loss contributed by TPA will be ~0.0004 dB/cm at 724 nm. If the optical power inside the waveguide is 100 mW, the nonlinear loss for the GaN waveguide will be ~0.04 dB/cm. For a SiN waveguide with similar dimensions, the loss is ~1 dB/cm at 720 nm.[26] (For GaN in the region where three photon absorption dominates, the nonlinear loss is only $\sim 10^{-7}$ dB/cm, which can be neglected. We also note that 100 mW is a very realistic value for optical power inside waveguide resonators to trigger the nonlinear process.) Therefore, GaN is potentially advantageous for the fabrication of the low loss waveguide in the near-infrared and visible spectrum regions. With even higher bandgap photon energy, a better performance can be expected on AlN waveguides.

TABLE I. Measured three-photon absorption coefficients for samples on the polar *c*-plane, nonpolar *m*-plane, and semipolar (20 $\bar{2}$1)-plane.

| | Three photon absorption coefficient $\gamma$ ($10^{-3}$ cm$^3$/GW$^2$) | | |
|---|---|---|---|
| Wavelength (nm) | *c*-plane | *m*-plane | (20$\bar{2}$1)-plane |
| 740 | 7.60 | 8.09 | 8.04 |
| 760 | 4.58 | 4.47 | 4.46 |
| 840 | 2.10 | 2.48 | 2.48 |

Finally, we also extracted the Kerr refractive index $n_{kerr}$ from closed aperture measurement, and the results are shown in Fig. 4. A theoretical model was used to fit the data.[23] The form of $n_{kerr}$ is given by $n_{kerr} = K' \frac{\sqrt{E_p}}{n_0 E_g^4} G_2(hbar \cdot \omega / E_g)$, where $E_g$, $E_p$, $n_0$, and $\omega$ have the same physical meaning as in Eq. (3). $K'$ is a material-independent constant related to $K$, and $G_2$ is the dispersion function. A detailed description can be found in Ref. 23. For simplicity, only TPA was considered in the dispersion function fitting. $n_{kerr}$ was characterized to be $\sim 2.50 \times 10^{-14}$ cm$^2$/W for all three samples on polar, nonpolar, and semipolar orientations. In previous studies, self-defocusing due to two-photon absorption and the quadratic stark effect were observed in GaN in visible and

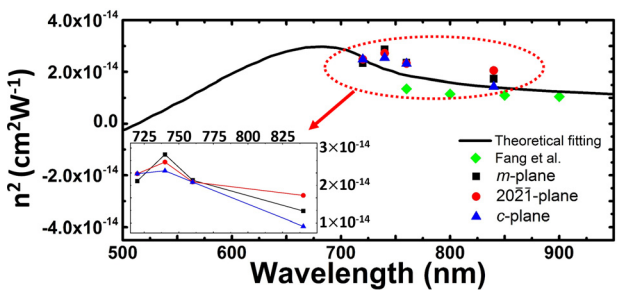


FIG. 4. Kerr refractive index vs. wavelength measured from the three samples. The theoretical fitting only considered the contribution by two-photon absorption.

near-UV regions.[16,27] In this study, however, a positive phase shift is observed, which is well predicted in Ref. 23 and recently also observed in Ref. 18. The high $n_{kerr}$ obtained in this work combined with the low β value makes the GaN material a promising candidate for the fabrication of all optical bistable switching waveguides.[28] Note that the optical nonlinearity is also related to crystal anisotropy, and more discussion can be found in Refs. 29 and 30.

In summary, we studied the basic nonlinear optical properties including TPA, 3PA, and Kerr refractive index for GaN on polar *c*-plane, nonpolar *m*-plane, and semipolar $(20\bar{2}1)$ plane bulk GaN crystals. No significant differences were observed for samples on these three orientations. Low TPA coefficients β (∼0.90 cm/GW at 724 nm and 0.65 cm/GW at 730 nm) were observed for GaN samples, which lead to very low nonlinear loss for GaN waveguide devices. For the Kerr refractive index, $n_{kerr} \sim 2.50 \times 10^{-14}\ \mathrm{cm}^2/\mathrm{W}$ was observed at 724 nm for all three samples. The results obtained in this work provide valuable information for the fabrication of high performance low loss GaN photonic devices and integrated photonic circuits, especially for the study of nonlinear processes inside high quality factor resonating structures (e.g., ring resonators and disk resonators).

This work was supported by the Bisgrove Scholar Program from Science Foundation Arizona. We gratefully acknowledge the use of facilities within the LeRoy Eyring Center for Solid State Science at Arizona State University. The author would like to thank Mengjia Zhu, Dr. Karl Weiss, Dr. Douglas Daniel, and Dr. Su Lin for the helpful assistance during the experiment.

[1]Y. Zhao, S. Tanaka, C. C. Pan, K. Fujito, D. Feezell, J. S. Speck, S. P. DenBaars, and S. Nakamura, Appl. Phys. Express **4**, 082104 (2011).
[2]Y. Zhao, Q. Yan, C. Y. Huang, S. C. Huang, P. S. Hsu, S. Tanaka, C. C. Pan, Y. Kawaguchi, K. Fujito, C. G. Van de Walle, and J. S. Speck, Appl. Phys. Lett. **100**, 201108 (2012).
[3]H. Fu, Z. Lu, X. H. Zhao, Y. H. Zhang, S. P. DenBaars, S. Nakamura, and Y. Zhao, J. Disp. Technol. **12**, 736 (2016).
[4]X. Huang, H. Fu, H. Chen, Z. Lu, D. Ding, and Y. Zhao, J. Appl. Phys. **119**, 213101 (2016).
[5]H. Chen, H. Fu, Z. Lu, X. Huang, and Y. Zhao, Opt. Express **24**, A856 (2016).
[6]H. Fu, Z. Lu, X. Huang, H. Chen, and Y. Zhao, J. Appl. Phys. **119**, 174502 (2016).
[7]H. Fu, H. Chen, X. Huang, Z. Lu, and Y. Zhao, J. Appl. Phys. **121**, 014501 (2017).
[8]M. Soltani, R. Soref, T. Palacios, and D. Englund, Opt. Express **24**, 25415 (2016).
[9]C. Xiong, W. Pernice, K. K. Ryu, C. Schuck, K. Y. Fong, T. Palacios, and H. X. Tang, Opt. Express **19**, 10462 (2011).
[10]H. Jung, C. Xiong, K. Y. Fong, X. Zhang, and H. X. Tang, Opt. Lett. **38**, 2810 (2013).
[11]Y. Okawachi, K. Saha, J. S. Levy, Y. H. Wen, M. Lipson, and A. L. Gaeta, Opt. Lett. **36**, 3398 (2011).
[12]X. Guo, C. L. Zou, C. Schuck, H. Jung, R. Cheng, and H. X. Tang, preprint arXiv:1603.03726 (2016).
[13]I. Roland, M. Gromovyi, Y. Zeng, M. El Kurdi, S. Sauvage, C. Brimont, T. Guillet, B. Gayral, F. Semond, J. Y. Duboz, M. de Micheli, X. Checoury, and P. Boucaud, Sci. Rep. **6**, 34191 (2016).
[14]I. Roland, Y. Zeng, X. Checoury, M. El Kurdi, S. Sauvage, C. Brimont, T. Guillet, B. Gayral, M. Gromovyi, J. Y. Duboz, and F. Semond, Opt. Express **24**, 9602 (2016).
[15]C. K. Sun, J. C. Liang, J. C. Wang, F. J. Kao, S. Keller, M. P. Mack, U. Mishra, and S. P. DenBaars, Appl. Phys. Lett. **76**, 439 (2000).
[16]V. Pacebutas, A. Stalnionis, A. Krotkus, T. Suski, P. Perlin, and M. Leszczynski, Appl. Phys. Lett. **78**, 4118 (2001).
[17]S. Petit, D. Guennani, P. Gilliot, C. Hirlimann, B. Hönerlage, O. Briot, and R. L. Aulombard, Mater. Sci. Eng., B **43**, 196 (1997).
[18]Y. Fang, Z. Xiao, X. Wu, F. Zhou, J. Yang, Y. Yang, and Y. Song, Appl. Phys. Lett. **106**, 251903 (2015).
[19]E. W. Van Stryland, H. Vanherzeele, M. A. Woodall, M. J. Soileau, A. L. Smirl, S. Guha, and T. F. Boggess, Opt. Eng. **24**, 244613 (1985).
[20]M. Sheik-Bahae, A. A. Said, T. H. Wei, D. J. Hagan, and E. W. Van Stryland, IEEE. J. Quantum Electron. **26**, 760 (1990).
[21]M. Funato, M. Ueda, Y. Kawakami, Y. Narukawa, T. Kosugi, M. Takahashi, and T. Mukai, Jpn. J. Appl. Phys., Part 1 **45**, L659 (2006).
[22]C. Y. Tsai, C. Y. Tsai, C. H. Chen, T. L. Sung, T. Y. Wu, and F. P. Shih, IEEE J. Quantum Electron. **34**, 552 (1998).
[23]M. Sheik-Bahae, D. C. Hutchings, D. J. Hagan, and E. W. Van Stryland, IEEE J. Quantum Electron. **27**, 1296 (1991).
[24]Y. Toda, T. Matsubara, R. Morita, M. Yamashita, K. Hoshino, T. Someya, and Y. Arakawa, Appl. Phys. Lett. **82**, 4714 (2003).
[25]S. Minissale, S. Yerci, and L. Dal Negro, Appl. Phys. Lett. **100**, 021109 (2012).
[26]A. Z. Subramanian, P. Neutens, A. Dhakal, R. Jansen, T. Claes, X. Rottenberg, F. Peyskens, S. Selvaraja, P. Helin, B. Du Bois, and K. Leyssens, IEEE Photonics J. **5**, 2202809 (2013).
[27]Y. L. Huang, C. K. Sun, J. C. Liang, S. Keller, M. P. Mack, U. K. Mishra, and S. P. DenBaars, Appl. Phys. Lett. **75**, 3524 (1999).
[28]A. Martínez, J. Blasco, P. Sanchis, J. V. Galán, J. García-Rupérez, E. Jordana, P. Gautier, Y. Lebour, S. Hernández, R. Spano, and R. Guider, Nano Lett. **10**, 1506 (2010).
[29]Y. Fang, F. Zhou, J. Yang, X. Wu, Z. Xiao, Z. Li, and Y. Song, Appl. Phys. Lett. **106**, 131903 (2015).
[30]K. Wang, J. Zhou, L. Yuan, Y. Tao, J. Chen, P. Lu, and Z. L. Wang, Nano Lett. **12**, 833 (2012).